Renormalization of the dephasing by zero point fluctuations

Swarnali Bandopadhyay[1,2] and Doron Cohen[1]
[1]*Department of Physics, Ben-Gurion University, Beer-Sheva 84105, Israel*
[2]*Max Planck Institute for the Physics of Complex Systems, Nöthnitzer Strasse 38, 01187 Dresden, Germany*
(Received 8 January 2008; revised manuscript received 28 March 2008; published 30 April 2008)

We study the role of zero point fluctuations (ZPF) in dephasing at low temperatures. Unlike the Caldeira–Leggett model, wherein the interaction is with a homogeneous fluctuating field of force, here we consider the effect of short range scattering by localized bath modes. We find that in the presence of ZPF, the inelastic cross section gets renormalized. Thus, ZPF might indirectly contribute to the dephasing at low temperatures.

DOI: 10.1103/PhysRevB.77.155438 PACS number(s): 03.65.Yz, 74.40.+k, 73.23.−b

I. INTRODUCTION

The coherent motion of a quantum mechanical particle in a fluctuating environment is endangered by decoherence due to inelastic scattering events. The temperature dependence of the resulting "dephasing" effect was worked out in numerous studies.[1–3] During the past decade, a controversy has emerged in the mesoscopic literature regarding the role of zero point fluctuations (ZPFs) in the theory of low temperature dephasing. The controversy was sparked by the experiment in Ref. 4, wherein a saturation of the dephasing rate in the limit of zero temperature was reported and, consequently, ZPF induced dephasing was suggested as an explanation[5] and was debated upon.[6–9]

Possibly, one can insist that a ZPF leads to "$T=0$" dephasing for a Brownian particle that interacts with an Ohmic Caldeira–Leggett (CL) bath,[10] wherein the fluctuations of the environment consist of long wavelength ($q=0$) modes. However,[11,12] in a metallic environment, the effective fluctuations are characterized by a finite correlation distance and, hence, consist of modes with wave numbers q that range up to the Fermi momentum. It was largely accepted[7,9] that if the interactions are short range, such that the fluctuations are characterized by a finite correlation distance, then the effect of the ZPF would be to renormalize the scattering cross section and the mass of the particle. It turns out that in the case of physical interest, particularly for the prototype model of Refs. 13 and 14, this renormalization effect is nondiverging in the zero temperature limit: both mass renormalization[15] and dephasing[16] for a single particle in the presence of a dirty metal environment have been studied. Essentially the same formulation as in Refs. 9 and 16 arises also in a more complicated many body treatment of the dephasing problem.[17]

Although it is not diverging in problems of physical interest, still the renormalization effect due to ZPF might be significant in the actual analysis. The simplest possibility is to have an overall suppression of both elastic and inelastic scattering via a *Debye–Waller factor* (DWF).[18] However, we would like to explore the more exotic possibility of having a distinct enhancement "factor" for the inelastic effect. It is therefore desired to have at least one exactly solvable model for dephasing due to short range scattering with environmental modes, which can be contrasted to the opposite CL limit, where all of the modes have $q=0$. The objective of the present paper is to present such a model: in the proposed model (see Fig. 1), the environment consists of infinitely many localized fluctuating modes with (say) an Ohmic spectral function, while the interaction is short range and described by $\delta(x)$ as in "s scattering." This should be contrasted to the long range interaction of the CL model, which is linear in x.

The outline of this paper is as follows: In Sec. II, we define a model for a localized bath that induces both ZPF and *thermal fluctuations* (TRFs). In Secs. III and IV, explicit expressions for its scattering matrix are derived following Ref. 19. In Secs. V and VI, low temperatures are considered, at which the TRFs are treated as a small perturbation. The example and the numerical analysis in Secs. VII and VIII establish that for a weak TRF, the effect of the ZPF background can be taken into account by defining a renormalized intensity of the TRF. Accordingly, ZPF may contribute to the dephasing at low temperatures, although not directly.

II. MODEL

The Hamiltonian of the particle plus the local bath is

$$\mathcal{H} = \frac{p^2}{2\mathsf{m}} + \delta(x)\sum_{\alpha} c_\alpha Q_\alpha + \sum_{\alpha} \hat{n}_\alpha \omega_\alpha. \qquad (1)$$

The index $n_\alpha=0,1,2,3,\ldots$, may indicate the state of the α oscillator, or optionally $n_\alpha=0$ and 1 may indicate the state of a two level ("spin") entity, as in our numerics. From now on, we use the notation

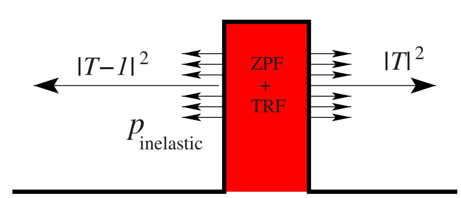

FIG. 1. (Color online) Schematic of the model system. The scattered wave of a particle that collides from the right with a thermal s scatterer consists of forward elastic scattering with an amplitude $\mathcal{T}$, backward elastic scattering with an amplitude $\mathcal{T}-1$, and isotropic inelastic scattering with a probability $p_{\text{inelastic}}$. Our purpose is to find the dependence of $\mathcal{T}$ and $p_{\text{inelastic}}$ on the intensity of the low temperature TRFs with an arbitrarily large background of ZPFs.

$$\hat{Q} = \sum_{\alpha} c_\alpha Q_\alpha. \quad (2)$$

By assuming an incident particle with a kinetic energy ϵ_k, we divide the oscillators into two groups: those with $\omega_\alpha < \epsilon_k$ and those with $\omega_\alpha > \epsilon_k$. We further assume low temperatures such that all of the oscillators in the latter group are in the ground state. Note that the particle has enough energy to induce real (nonvirtual) excitation of any of the TRF oscillators. Hence, we can schematically write the following:

$$\hat{Q} = c_S + \sum_{\alpha\in\mathrm{ZPF}} c_\alpha Q_\alpha + \sum_{\alpha\in\mathrm{TRF}} c_\alpha Q_\alpha, \quad (3)$$

where c_S represents a static scatterer. The particle is affected by the fluctuations in Q. By assuming that the bath is prepared in the state $n=m$, the fluctuations are characterized by the following nonsymmetrized power spectrum:

$$\tilde{S}(\omega) = \overline{\sum_{n(\neq m)} |Q_{nm}|^2 2\pi\delta[\omega - (E_n - E_m)]}. \quad (4)$$

In Sec. III, we show how the ZPF oscillators can be eliminated, such that the interaction is characterized by a dressed interaction matrix $\mathcal{Q}$. Accordingly, we define the effective power spectrum as

$$\tilde{S}_{\mathrm{eff}}(\omega) = \overline{\sum_{n(\neq m)} |\mathcal{Q}_{nm}|^2 2\pi\delta[\omega - (E_n - E_m)]} \quad (5)$$

and the *effective* "size" of the elastic scatterer as

$$c_{\mathrm{eff}} = \mathcal{Q}_{m,m}. \quad (6)$$

In the following sections, we will explain how to define $\mathcal{Q}$ and how to make the exact calculation of the elastic scattering amplitude $\mathcal{T}$ and of the inelastic scattering cross section $p_{\mathrm{inelastic}}$ (see Fig. 1). Then, we discuss whether the results can be deduced from the effective values of c_{eff} and $\tilde{S}_{\mathrm{eff}}(\omega)$.

III. SCATTERING STATES

Outside of the scattering region, the total energy of the system (particle plus bath) is

$$\mathcal{E} = \epsilon_k + E_n = \epsilon_k + \sum_\alpha n_\alpha \omega_\alpha. \quad (7)$$

We look for scattering states that satisfy the equation

$$\mathcal{H}|\Psi\rangle = \mathcal{E}|\Psi\rangle.$$

Open (propagating) channels are those for which $\epsilon_k > 0$ after scattering. Otherwise, the channels are closed (evanescent). The channels are labeled as

$$\boldsymbol{n} = (n_0, n) = (n_0, n_{\mathrm{ZPF}}, n_{\mathrm{TRF}}) = (n_0, n_1, n_2, n_3, \ldots, n_\alpha, \ldots), \quad (8)$$

where n_0=L,R for left/right, and $n_{\mathrm{ZPF}}, n_{\mathrm{TRF}}$ are collective indices for the two group of scatterers. We define the following:

$$k_{\boldsymbol{n}} = \sqrt{2m(\mathcal{E} - E_n)} \quad \text{for } n \in \text{open}, \quad (9)$$

$$\alpha_{\boldsymbol{n}} = \sqrt{-2m(\mathcal{E} - E_n)} \quad \text{for } n \in \text{closed}. \quad (10)$$

Later, we use the notations

$$v_{\boldsymbol{n}} = k_{\boldsymbol{n}}/\mathbf{m}, \quad (11)$$

$$u_{\boldsymbol{n}} = \alpha_{\boldsymbol{n}}/\mathbf{m}, \quad (12)$$

and define diagonal matrices $\boldsymbol{v}=\mathrm{diag}\{v_n\}$ and $\boldsymbol{u}=\mathrm{diag}\{u_n\}$. The channel radial functions are written as follows:

$$R(r) = A_n e^{-ik_n r} + B_n e^{+ik_n r}, \quad n \in \text{open}, \quad (13)$$

$$R(r) = C_n e^{-\alpha_n r}, \quad n \in \text{closed}, \quad (14)$$

where $r=|x|$. The wave function can be written as

$$\Psi(r, n_0, Q) = \sum_n R_{n_0,n}(r)\chi^n(Q). \quad (15)$$

The matching equations are

$$\Psi(0,\mathrm{right},Q) - \Psi(0,\mathrm{left},Q) = 0, \quad (16)$$

$$\frac{1}{2\mathbf{m}}[\Psi'(0,\mathrm{right},Q) + \Psi'(0,\mathrm{left},Q)] = \hat{Q}\Psi(0,Q). \quad (17)$$

The operator $\hat{Q}$ is represented by the matrix Q_{nm} that has the following block structure:

$$Q_{nm} = \begin{pmatrix} Q_{vv} & Q_{vu} \\ Q_{uv} & Q_{uu} \end{pmatrix}. \quad (18)$$

The matching conditions lead to the following set of matrix equations:

$$A_R + B_R = A_L + B_L,$$

$$C_R = C_L,$$

$$-i\boldsymbol{v}(A_R - B_R + A_L - B_L) = 2Q_{vv}(A_L + B_L) + 2Q_{vu}C_L,$$

$$-\boldsymbol{u}(C_R + C_L) = 2Q_{uv}(A_L + B_L) + 2Q_{uu}C_L.$$

From here, we get the following matching equations that relate the ingoing and the outgoing amplitudes:

$$A_R + B_R = A_L + B_L, \quad (19)$$

$$A_R - B_R + A_L - B_L = i2(\boldsymbol{v})^{-1}\mathcal{Q}(A_L + B_L), \quad (20)$$

where the dressed interaction matrix is defined as

$$\mathcal{Q} = Q_{vv} - Q_{vu}\frac{1}{(\boldsymbol{u} + Q_{uu})}Q_{uv}. \quad (21)$$

In Sec. IV, we deduce the $\boldsymbol{S}$ matrix from the above set of equations and obtain explicit expressions for the elastic scattering amplitude and inelastic cross section.

IV. *S* MATRIX

The unitary description of the scattering in terms of ingoing and outgoing probability currents requires defining the normalized ingoing and outgoing amplitudes as $\widetilde{A}_n = \sqrt{v_n} A_n$ and $B_n = \sqrt{v_n} B_n$. Consequently, we defined a rescaled version of the Q_{nm} matrix as follows:

$$M_{nm} = \begin{pmatrix} M_{vv} & M_{vu} \\ M_{uv} & M_{uu} \end{pmatrix} = \begin{pmatrix} \frac{1}{\sqrt{v}} Q_{vv} \frac{1}{\sqrt{v}} & \frac{1}{\sqrt{v}} Q_{vu} \frac{1}{\sqrt{u}} \\ \frac{1}{\sqrt{u}} Q_{uv} \frac{1}{\sqrt{v}} & \frac{1}{\sqrt{u}} Q_{uu} \frac{1}{\sqrt{u}} \end{pmatrix}. \tag{22}$$

We also define a corresponding reduced matrix as follows:

$$\mathcal{M} = \frac{1}{\sqrt{\boldsymbol{v}}} \mathcal{Q} \frac{1}{\sqrt{\boldsymbol{v}}} = M_{vv} - M_{vu} \frac{1}{1 + M_{uu}} M_{uv}. \tag{23}$$

By using these notations, the set of matching conditions can be expressed by using a transfer matrix as follows:

$$\begin{pmatrix} \widetilde{B}_R \\ \widetilde{A}_R \end{pmatrix} = \boldsymbol{T} \begin{pmatrix} \widetilde{A}_L \\ \widetilde{B}_L \end{pmatrix}. \tag{24}$$

The transfer $2N \times 2N$ matrix can be written in block form as follows:

$$\boldsymbol{T} = \begin{pmatrix} \boldsymbol{T}_{++} & \boldsymbol{T}_{+-} \\ \boldsymbol{T}_{-+} & \boldsymbol{T}_{--} \end{pmatrix} = \begin{pmatrix} 1 - i\mathcal{M} & -i\mathcal{M} \\ i\mathcal{M} & 1 + i\mathcal{M} \end{pmatrix}. \tag{25}$$

The $\boldsymbol{S}$ matrix is defined via

$$\begin{pmatrix} \widetilde{B}_L \\ \widetilde{B}_R \end{pmatrix} = \boldsymbol{S} \begin{pmatrix} \widetilde{A}_L \\ \widetilde{A}_R \end{pmatrix} \tag{26}$$

and can be written in block form as

$$\boldsymbol{S}_{\boldsymbol{n},\boldsymbol{m}} = \begin{pmatrix} \boldsymbol{S}_R & \boldsymbol{S}_T \\ \boldsymbol{S}_T & \boldsymbol{S}_R \end{pmatrix}. \tag{27}$$

A straightforward elimination gives

$$\boldsymbol{S} = \begin{pmatrix} -\boldsymbol{T}_{--}^{-1}\boldsymbol{T}_{-+} & \boldsymbol{T}_{--}^{-1} \\ \boldsymbol{T}_{++} - \boldsymbol{T}_{-+}\boldsymbol{T}_{--}^{-1}\boldsymbol{T}_{+-} & \boldsymbol{T}_{+-}\boldsymbol{T}_{--}^{-1} \end{pmatrix}. \tag{28}$$

Now we can write the following expressions for $\boldsymbol{S}_R$ and $\boldsymbol{S}_T$ by using the $\mathcal{M}$ matrix:

$$\boldsymbol{S}_T = \frac{1}{1 + i\mathcal{M}} = 1 - i\mathcal{M} - \mathcal{M}^2 + i\mathcal{M}^3 + \cdots, \tag{29}$$

$$\boldsymbol{S}_R = \boldsymbol{S}_T - \boldsymbol{1}. \tag{30}$$

The elastic forward scattering amplitude is

$$\mathcal{T} = [\boldsymbol{S}_T]_{\boldsymbol{m},\boldsymbol{m}} = \left[\frac{1}{1 + i\mathcal{M}} \right]_{\boldsymbol{m},\boldsymbol{m}}. \tag{31}$$

The total elastic scattering probability is

$$p_{\text{elastic}} = |\mathcal{T}|^2 + |\mathcal{T} - 1|^2 = 1 - 2[\Re(\mathcal{T}) - |\mathcal{T}|^2]. \tag{32}$$

We observe that the inelastic scattering is isotropic and its line shape (per direction) is

$$p(\omega) = \sum_{\boldsymbol{n}(\neq \boldsymbol{m})} |[\boldsymbol{S}_T]_{\boldsymbol{nm}}|^2 2\pi\delta[\omega - (E_{\boldsymbol{n}} - E_{\boldsymbol{m}})], \tag{33}$$

with the measurement $d\omega/2\pi$. The total inelastic cross section is obtained by integration as follows:

$$p_{\text{inelastic}} = 2\int \frac{d\omega}{2\pi} p(\omega) = 2 \sum_{\boldsymbol{n}(\neq \boldsymbol{m})} |[\boldsymbol{S}_T]_{\boldsymbol{n},\boldsymbol{m}}|^2 = 2 \sum_{\boldsymbol{n}(\neq \boldsymbol{m})} \left| \left[\frac{1}{1 + i\mathcal{M}} \right]_{\boldsymbol{n},\boldsymbol{m}} \right|^2. \tag{34}$$

One can verify that $p_{\text{inelastic}}$ and p_{elastic} sum up to unity, which is essentially the "optical theorem."

V. PERTURBATION THEORY

Since the temperature is low, we treat the small effect of the TRF in leading order. We write

$$\hat{Q} = \hat{Q}^{\text{ZPF}} \otimes \boldsymbol{1}^{\text{TRF}} + \boldsymbol{1}^{\text{ZPF}} \otimes \hat{Q}^{\text{TRF}} \equiv \hat{Q}^0 + \delta\hat{Q}, \tag{35}$$

where $\hat{Q}^0$ is the sum over the ZPF coordinates including the static scatterer c_{S}, while $\delta\hat{Q}$ is the sum over the TRF coordinates. For the reduced $\mathcal{Q}$ matrix, we get

$$\mathcal{Q} = Q_{vv}^0 + \delta Q_{vv} - Q_{vu}^0 \left(\frac{1}{\boldsymbol{u} + Q_{uu}^0} - \frac{1}{\boldsymbol{u} + Q_{uu}^0} \delta Q_{uu} \frac{1}{\boldsymbol{u} + Q_{uu}^0} \right) Q_{uv}^0. \tag{36}$$

We assume that all of the "important" open modes are well above the evanescent threshold. This means that a single TRF transition is not enough to push the scattered particle into an evanescent mode. Accordingly, δQ_{uv} and δQ_{vu} are not included. In the same spirit, we further assume that the TRF transitions hardly affect the evanescent velocity; hence,

$$u_{n_{\text{ZPF}}, n_{\text{TRF}}} \approx u_{n_{\text{ZPF}}, 0}. \tag{37}$$

When calculating the matrix element $\mathcal{Q}_{\boldsymbol{nm}}$, the second term constitutes a sum over sequences as $Q_{n,\nu}^0 \ldots (\delta Q)_{\nu',\mu'} \ldots Q_{\mu,m}^0$. To have a nonzero term, the TRF oscillators of the ν state should remain in the same state as in the n state, while one ZPF oscillator of the ν state has to be excited. A similar observation applies to the states of the oscillators of the μ state. The TRF transitions are induced by δQ during the evanescent motion of the particle. Accordingly, we deduce that

$$\mathcal{Q} = \left(\left[Q_{vv}^{\text{ZPF}} - Q_{vu}^{\text{ZPF}} \left(\frac{1}{\boldsymbol{u} + Q_{uu}^{\text{ZPF}}} \right) Q_{uv}^{\text{ZPF}} \right]_{m,m} \right) \boldsymbol{1}^{\text{TRF}} + \left(1 + \left[Q_{vu}^{\text{ZPF}} \left(\frac{1}{\boldsymbol{u} + Q_{uu}^{\text{ZPF}}} \right)^2 Q_{uv}^{\text{ZPF}} \right]_{m,m} \right) Q^{\text{TRF}},$$

which can be written schematically as follows:

$$\mathcal{Q} = c_0 \boldsymbol{1}^{\text{TRF}} + \lambda_0 Q^{\text{TRF}}, \tag{38}$$

where the effective elastic scattering amplitude and the scaling factor of the inelastic effect are

$$c_0 = c_{\text{S}} - \left[Q_{vu}^{\text{ZPF}} \left(\frac{1}{\boldsymbol{u} + Q_{uu}^{\text{ZPF}}} \right) Q_{uv}^{\text{ZPF}} \right]_{m,m}, \tag{39}$$

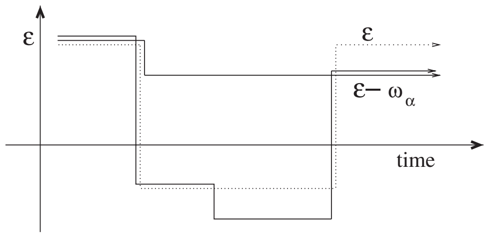

FIG. 2. Diagrams that describe the time evolution of kinetic energy can be used in order to illustrate the terms in the scattering calculation. The dotted line represents a contribution to the elastic cross section due to (virtual) scattering by ZPF modes. The solid lines represent contributions to the first order inelastic cross section, wherein the intensity of the TRF is regarded as the small parameter.

$$\lambda_0 = 1 + \left[Q^{\text{ZPF}}_{vu} \left(\frac{1}{\boldsymbol{u} + Q^{\text{ZPF}}_{uu}} \right)^2 Q^{\text{ZPF}}_{uv} \right]_{m,m}. \tag{40}$$

With an appropriate counterterm, we can make $c_0 = 0$. More interestingly, we see that the effective TRFs are characterized by the dressed power spectrum as follows:

$$\tilde{S}_{\text{eff}}(\omega) = (\lambda_0)^2 \tilde{S}(\omega). \tag{41}$$

VI. DRESSED BORN APPROXIMATION

The first order ("Born") approximation relates the inelastic line shape to the power spectrum of the fluctuations. We use the term "dressed Born approximation" to indicate that we use a first order perturbation theory with respect to the TRF, while the ZPF including the static scatterer are treated to infinite order (Fig. 2). Within this framework, the leading order expression for the $\boldsymbol{S}$ matrix, by using Eqs. (38)–(40), is

$$\boldsymbol{S}_T \approx \frac{1}{1 + i(c_0/v_\epsilon) + i\lambda_0 \mathcal{M}^{\text{TRF}}} = \mathcal{T}_0 \mathbf{1} - i\mathcal{T}_0^2 \lambda_0 \mathcal{M}^{\text{TRF}} + \cdots, \tag{42}$$

where the elastic forward scattering amplitude is

$$\mathcal{T}_0 = \frac{1}{1 + i(c_0/v_\epsilon)}. \tag{43}$$

Consequently, for the inelastic scattering, we get

$$p(\omega) \approx \frac{1}{v_\epsilon v_{\epsilon-\omega}} |\mathcal{T}_0|^4 (\lambda_0)^2 \tilde{S}(\omega). \tag{44}$$

Since we have assumed that the change in the kinetic energy of the particle due to TRF inelastic scattering is relatively small, one can take $v_{\epsilon-\omega} \approx v_\epsilon$.

VII. SIMPLEST EXAMPLE

Consider a particle with a velocity v_ϵ that collides with a "bath" that consists of an elastic scatterer c_{S} and a single two level TRF scatterer c_{T}, whose excitation energy is $\omega_{\text{T}} (\ll \epsilon_k)$. The interaction matrix is

$$\mathcal{Q} = Q = \begin{pmatrix} c_S & c_T \\ c_T & c_S \end{pmatrix}, \tag{45}$$

which we substitute in $\mathcal{M} \approx (1/v_\epsilon)^2 \mathcal{Q}$ so as to get $\boldsymbol{S}_T = (1 + i\mathcal{M})^{-1}$. To avoid crowded expressions, we set the units such that $v_\epsilon = 1$ and write

$$\boldsymbol{S}_T = \frac{1}{(1 + ic_S)^2 + c_T^2} \begin{pmatrix} 1 + ic_S & -ic_T \\ -ic_T & 1 + ic_S \end{pmatrix}. \tag{46}$$

(Note again that in order to restore the units, each c in the above expression should be replaced with c/v_ϵ.) From here, it follows that

$$p_{\text{inelastic}} = \frac{2\nu_{\text{TRF}}}{(1 - c_0^2 + \nu_{\text{TRF}})^2 + 4c_0^2} \quad \text{(scaled)}, \tag{47}$$

where $\nu_{\text{TRF}} \equiv c_T^2$ characterizes the intensity of the TRF and $c_0 \equiv c_S$. One observes that for a strong TRF, the inelastic effect is suppressed and we get mainly elastic back reflection. However, in the regime of interest, of a weak TRF, the inelastic scattering is proportional to νTRF and agree with Eq. (44), where $|\mathcal{T}_0|^2 = 1/(1 + c_0^2)$ and $\lambda_0 = 1$.

Next, we complicate the bath by adding a single ZPF scatterer c_Z, whose excitation energy is $\omega_Z (> \epsilon_k)$. The possible values of the mode index are $n = (0,0) \equiv 1$, $n = (0,1) \equiv 2$, $n = (1,0) \equiv 3$, and $n = (1,1) \equiv 4$. The ZPF scatterer is assumed to be in the ground state ($m = 1$) and, hence, only the first two modes are open. The interaction matrix is

$$Q = \begin{pmatrix} c_S & c_T & c_Z & 0 \\ c_T & c_S & 0 & c_Z \\ c_Z & 0 & c_S & c_T \\ 0 & c_Z & c_T & c_S \end{pmatrix}.$$

If we did not have the TRF oscillator, it would be a 2×2 matrix as follows:

$$Q^{\text{ZPF}} = \begin{pmatrix} c_S & c_Z \\ c_Z & c_S \end{pmatrix}. \tag{48}$$

If we ignored the ZPF oscillator, we would get Eq. (45). However, by using Eq. (21), we get the dressed interaction matrix as follows:

$$\mathcal{Q} = \begin{pmatrix} c_S & c_T \\ c_T & c_S \end{pmatrix} - \frac{c_Z^2}{(u_3 + c_S)(u_4 + c_S) - c_T^2} \times \begin{pmatrix} (u_3 + c_S) & -c_T \\ -c_T & (u_4 + c_S) \end{pmatrix},$$

with $u_3 = \sqrt{|\epsilon_k - \omega_Z|}$ and $u_4 = \sqrt{|\epsilon_k - \omega_Z - \omega_T|}$. Consequently, from $c_{\text{eff}} \equiv \mathcal{Q}_{1,1}$, we get

$$c_{\text{eff}} = c_S - \frac{(u_3 + c_S)\nu_{\text{ZPF}}}{(u_3 + c_S)(u_4 + c_S) - \nu_{\text{TRF}}}, \tag{49}$$

and from $\nu_{\text{eff}} \equiv |\mathcal{Q}_{2,1}|^2$, we get $\nu_{\text{eff}} = \lambda^2 \nu_{\text{TRF}}$, where

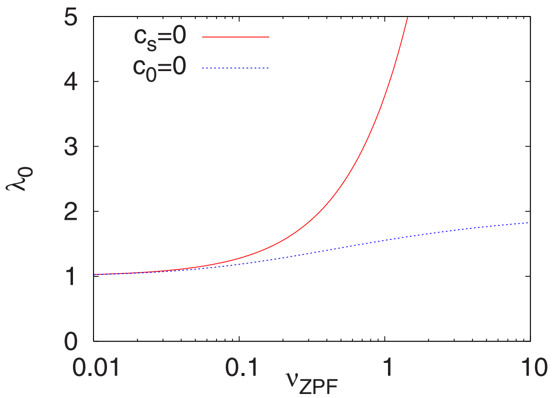

FIG. 3. (Color online) The renormalization factor for inelastic effect λ_{ZPF} is plotted as a function of ν_{ZPF} for the simple model of Sec. VII by using Eq. (52) with a fixed static scatterer $c_S=0$ (solid red curve) and with an adaptive static scatterer such that $c_0=0$ (dashed blue curve). The other parameters for this and for the next figures are $\omega_Z=0.96$ and $\omega_T=0.03$ and $\epsilon_k=0.6$, respectively.

$$\lambda = 1 + \frac{\nu_{\text{ZPF}}}{(u_3+c_S)(u_4+c_S) - \nu_{\text{TRF}}}, \quad (50)$$

where $\nu_{\text{ZPF}} \equiv c_Z^2$ and $\nu_{\text{TRF}} \equiv c_T^2$. Optionally, we can get for $\mathcal{Q}$ the approximated result of Eq. (38), which treats the TRF coupling in leading order. This treatment assumes that in the vicinity of the energy shell, $v_1 \approx v_2 \equiv v_\epsilon$ and $u_3 \approx u_4 \equiv u_Z$. The parameters c_0 and λ_0 are calculated by using Eqs. (39) and (40) with $Q_{uu}^{\text{ZPF}} = c_S$ and $Q_{vu}^{\text{ZPF}} = Q_{uv}^{\text{ZPF}} = c_Z$, which leads to

$$c_0 = c_S - \frac{\nu_{\text{ZPF}}}{(u_Z+c_S)}, \quad (51)$$

$$\lambda_0 = 1 + \frac{\nu_{\text{ZPF}}}{(u_Z+c_S)^2}. \quad (52)$$

In this simple example, the dependence of c_0 and λ_0 on ν_{ZPF} is linear. However, once we have more than one ZPF scatterer (as in the numerical example in Sec. VIII), the relation is no longer linear. It might also be of interest to solve the first equation $c_0=0$ for c_S, and substitute the result into the second equation. The outcome of this procedure is illustrated in Fig. 3.

The calculation of the ***S*** matrix proceeds in the same way as in the single TRF case, with the effective interaction matrix (no approximation involved) as follows:

$$\mathcal{Q} = \begin{pmatrix} c_S - (\lambda-1)(u_3+c_S) & \lambda c_T \\ \lambda c_T & c_S - (\lambda-1)(u_4+c_S) \end{pmatrix}. \quad (53)$$

By setting $v_1 \approx v_2 \equiv v_\epsilon$ and $u_3 \approx u_4 \equiv u_Z$ as before, we label both diagonal terms as c_{eff}. Still we are not making any approximation with regard to the intensities ν_{TRF} and ν_{ZPF}, so as to get essentially exact results as follows:

$$|\mathcal{T}|^2 = \frac{[v_\epsilon^2 + (c_{\text{eff}})^2]v_\epsilon^2}{[v_\epsilon^2 - (c_{\text{eff}})^2 + \lambda^2\nu_{\text{TRF}}]^2 + 4v_\epsilon^2(c_{\text{eff}})^2} \quad (54)$$

and the generalization of Eq. (47) as follows:

$$p_{\text{inelastic}} = \frac{2}{v_\epsilon^2}|\tilde{\mathcal{T}}|^2|\mathcal{T}|^2\lambda^2\nu_{\text{TRF}}, \quad (55)$$

where $|\tilde{\mathcal{T}}|^2$ is Eq. (54) without the $\lambda^2\nu_{\text{TRF}}$ term. For a weak TRF intensity, by using $\lambda \approx \lambda_0$ and $\mathcal{T} \approx \mathcal{T}_0$, one obtains the dressed Born approximation [Eq. (44)]. One observes that the presence of the factor λ has two implications: one is to enhance the inelastic scattering for a weak TRF, while the other is to limit the range over which the weak TRF approximation applies.

VIII. DISCUSSION, EXPECTATIONS, AND NUMERICAL DEMONSTRATION

The analysis in the present paper is focused primarily on the low temperature scattering, due to a weak TRF, where the dressed Born approximation of Sec. VI applies. Still, to get the "big picture," we consider below the full range of ν_{TRF} values. We first highlight some qualitative observations that are based on the analysis of the simple examples of Sec. VII, and then proceed with a numerical demonstration that involves a larger bath of scatterers.

From the Born approximation, we deduce that for a weak TRF, the inelastic cross section $p_{\text{inelastic}}$ is proportional to ν_{TRF}. For a strong TRF, it drops down as implied, e.g., by the simplest example Eq. (47). The maximum $p_{\text{inelastic}}=1/2$ is attained for the intermediate value $\nu_{\text{TRF}}=c_0^2+1$. *A priori* we could not expect a larger inelastic effect because the elastic cross section $|\mathcal{T}|^2+|\mathcal{T}-1|^2$ is bound from below by the minimum value of 50%. We can interpret the condition for attaining a minimum elastic cross section by using a Fabry–Pérot double barrier picture: the elastic scattering and the inelastic scattering are like two barriers separated by an infinitesimal distance. The strongest interference effect is expected when the two barriers are comparable.

The suppression of the inelastic effect for strong TRF is a generic effect: it becomes almost obvious if we consider the scattering of a particle from a fluctuating region in a three-dimensional space. In the latter context, strong fluctuations would repel the particle from the scattering region, hence, making inelastic excitations within the excluded volume less likely. So the strongest inelastic effect is experienced for intermediate values of ν_{TRF}.

The inclusion of ZPF into the model renormalizes ν_{TRF}. The enhancement factor λ is larger than unity (but finite) in the Born approximation limit, but if we go to very high temperatures (large ν_{TRF}), this renormalization effect fades away and we get $\lambda=1$ [see, e.g., Eq. (50)]. The crossover involves a wild variation in λ (see Fig. 4), which implies that $0<p_{\text{inelastic}}<1/2$ goes through the whole range of possible values (Fig. 5).

It is important to point out that if the fluctuations had a continuous (rather than discrete) power spectrum, the above described intermediate wild variation would be smoothed

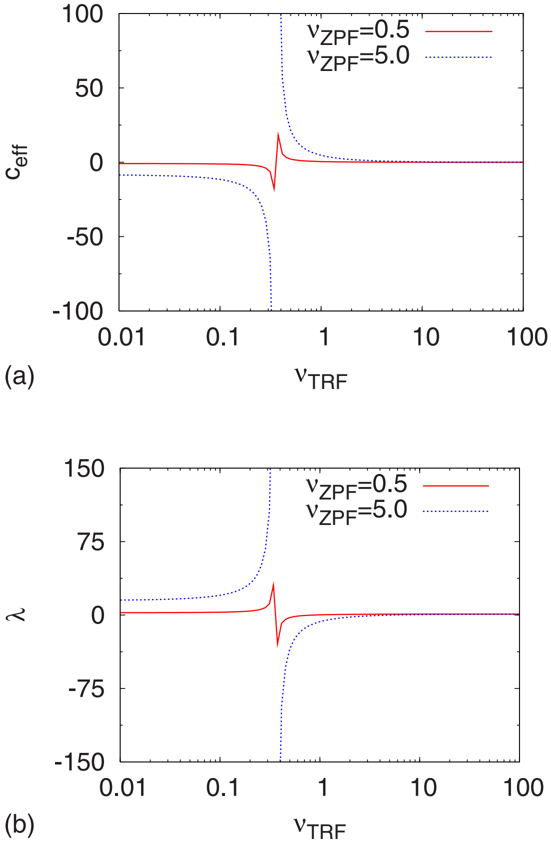

FIG. 4. (Color online) Plots of c_{eff} (upper panel) and λ (lower panel) versus ν_{TRF} for the simple model of Sec. VII, with the same parameters as in Fig. 3. The red solid curves are for ν_{ZPF}=0.5 and the blue dashed curves are for ν_{ZPF}=5.

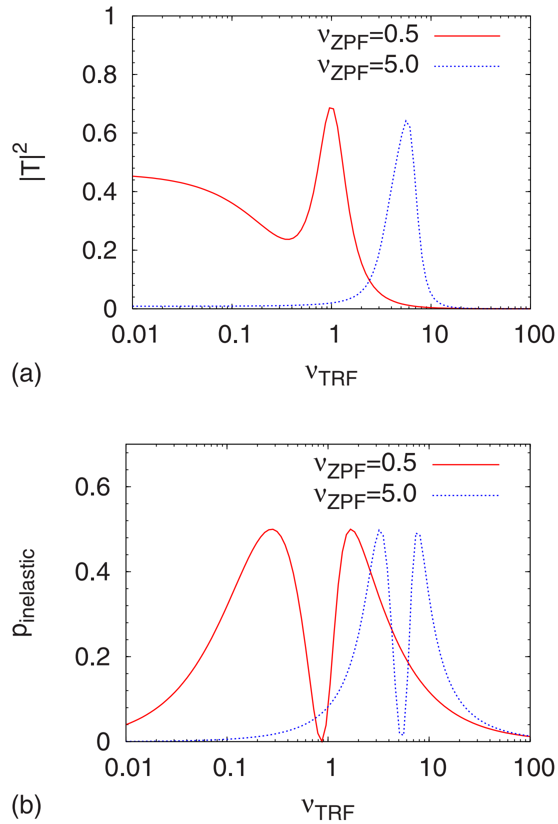

FIG. 5. (Color online) The transmission $|\mathcal{T}|^2$ (upper panel) and the inelastic cross section $p_{\text{inelastic}}$ (lower panel) versus ν_{TRF} for the simple model of Sec. VII, with the same parameters as in Figs. 3 and 4.

away. Thus, in realistic circumstances, we expect that also in the presence of ZPF, the qualitative dependence of $p_{\text{inelastic}}$ on ν_{TRF} would be smooth, although renormalized by λ_0 at the limit of low temperatures.

For the numerical study, we consider a bath that consists of two level scatterers. The energy splitting of the α scatterer is ω_α, and the interaction is described by the operator

$$Q_\alpha = \begin{pmatrix} 0 & 1 \\ 1 & 0 \end{pmatrix}.$$

The strength of the interaction with the bath is characterized by the intensity of the fluctuations as obtained by integrating over their power spectrum $\tilde{S}(\omega)$. Consequently, we distinguish between the intensity of the ZPF and the intensity of the TRF as follows:

$$\nu_{\text{ZPF}} = \sum_{\alpha \in \text{ZPF}} c_\alpha^2, \tag{56}$$

$$\nu_{\text{TRF}} = \sum_{\alpha \in \text{TRF}} c_\alpha^2. \tag{57}$$

The effective intensity of the thermal fluctuations is similarly defined and accordingly calculated from the dressed interaction matrix as follows:

$$\nu_{\text{eff}} = \sum_{n(\neq m)} |\mathcal{Q}_{n,m}|^2. \tag{58}$$

Given a set of N ZPF scatterers with couplings c_Z and a static scatterer c_S, we calculate c_0 (which determines $\mathcal{T}_0$) and λ_0 as a function of $\nu_{\text{ZPF}} \equiv N|c_Z|^2$ (see Fig. 6). Then, for various values of ν_{ZPF}, we calculate the exact results for ν_{eff} and $p_{\text{inelastic}}$ versus ν_{TRF} (see Fig. 7). One expects that for weak TRF, the effective intensity ν_{eff} would be proportional to ν_{TRF}, namely,

$$\nu_{\text{eff}} \approx (\lambda_0)^2 \nu_{\text{TRF}}. \tag{59}$$

Furthermore, our perturbative scheme implies that

$$p_{\text{inelastic}} \approx \frac{2}{v_\epsilon^2} |\mathcal{T}|^4 \nu_{\text{eff}}. \tag{60}$$

To test the quality of the latter approximation, we replot the results for $p_{\text{inelastic}}$ versus $|\mathcal{T}|^4 \nu_{\text{eff}}$ (see Fig. 8). The numerical results confirm our qualitative expectations and are in agreement with the analysis of the simple example of Sec. VII. In particular, one observes that the presence of ZPF has two implications: one is to enhance the inelastic scattering for a weak TRF, while the other is to limit the range over which the weak TRF approximation applies.

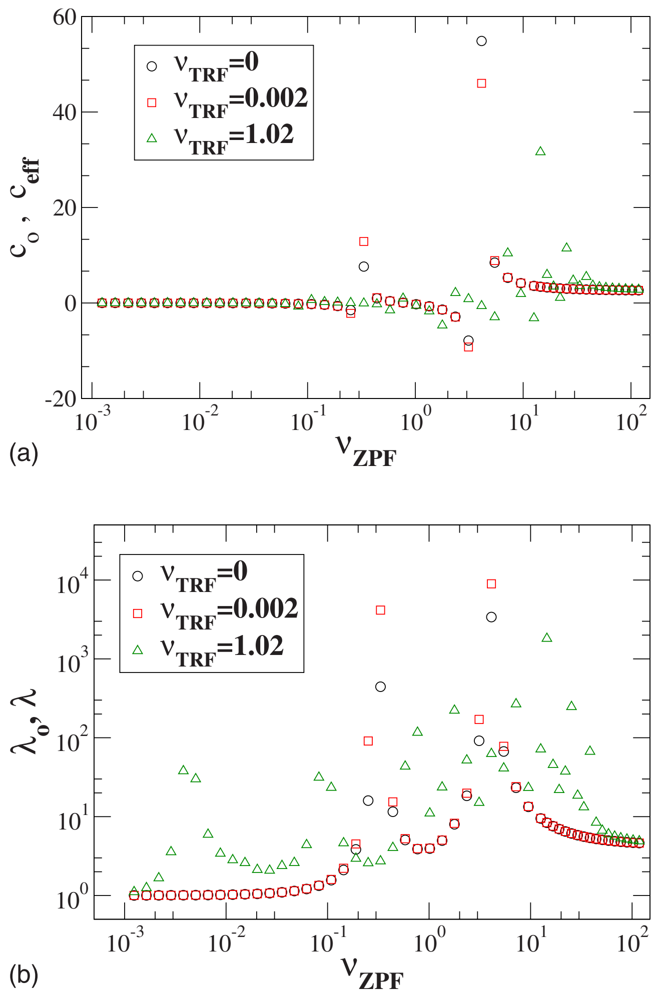

FIG. 6. (Color online) Plots of c_0 and λ_0 versus ν_{ZPF}. For the sake of comparison, we also plot c_{eff} and $\lambda \equiv (\nu_{\mathrm{eff}}/\nu_{\mathrm{TRF}})^{1/2}$ for two nonzero values of ν_{TRF}. Here and in Fig. 7, we consider a bath that consists of seven TRF scatterers with $\omega_\alpha \sim 0.0003$ and four ZPF scatterers with $\omega_\alpha \sim 0.96$. There is no static scatterer ($c_S=0$). The kinetic energy of the incident particle is $\epsilon_k=0.6$.

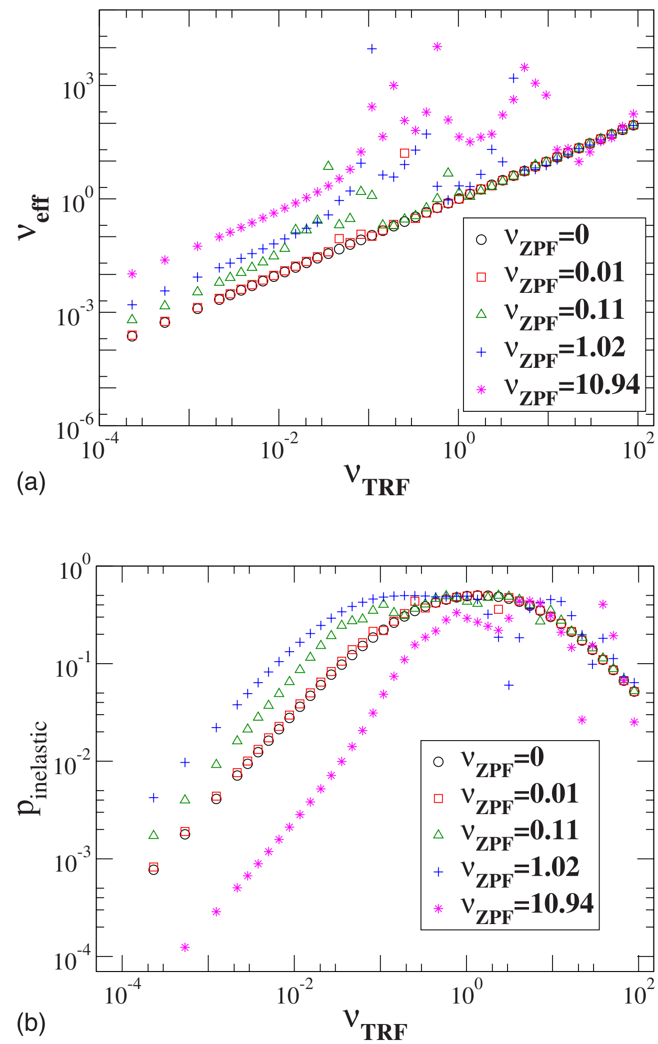

FIG. 7. (Color online) Plots of ν_{eff} and $p_{\mathrm{inelastic}}$ versus ν_{TRF} for the same bath as in Fig. 6.

IX. SUMMARY

In the Caldeira–Leggett model, the effect of the environment is characterized by a friction coefficient η and by a temperature T. However, more generally,[9,11,12,16] it has been emphasized that the proper way to characterize the environment is by its form factor $\tilde{S}(q,\omega)$. The form factor contains information on both the temporal and the spatial aspects of the fluctuations and, in particular, one can extract from it not only T and η but also the spatial correlations. The general formula for the rate of dephasing[9,16] involves a $dqd\omega$ integral over $\tilde{S}(q,\omega)$ and, for short range interactions, simply reflect the rate of inelastic events.

We find for our model system that the inelastic scattering cross section $p_{\mathrm{inelastic}}$ is enhanced in the presence of ZPF and, accordingly, ZPF may contribute to the dephasing at low temperatures, although indirectly. This might come as a surprise since in Ref. 18 it was argued that both elastic and inelastic scatterings are suppressed by ZPF by the *same* DWF. A closer look reveals the difference between the two models involved. In Ref. 18, one considers the scattering of a particle ($\hat{x}$) from a vibrating scatterer ($\hat{Q}$), where the interaction is $\delta(\hat{x}-\hat{Q})$. Accordingly, the particle experiences a fluctuating field $\hat{\mathcal{U}}(x)=\delta(\hat{Q}-x)$, and $\tilde{S}(q,\omega)$ is the Fourier transform of $\langle e^{-iq\hat{Q}(t)}e^{iq\hat{Q}(0)}\rangle$, which is suppressed by the DWF $e^{-\langle \hat{Q}^2 q^2\rangle}$. In our model, the interaction is $\delta(\hat{x})\hat{Q}$. Accordingly, $\tilde{S}(q,\omega)$ is the Fourier transform of $\langle \hat{Q}(t)\hat{Q}(0)\rangle$, and within the framework of the conventional Born approximation, there is no DWF involved: in our model, adding high frequency components to the fluctuating field has no implication on the low frequency behavior of $\tilde{S}(q,\omega)$.

The renormalization factor of the inelastic effect (λ) in our *dressed* Born approximation comes from higher orders of the perturbation theory with respect to the ZPF, while the TRF is treated in leading order. The renormalization factor λ multiplies the power spectrum $\tilde{S}(\omega)$ that describes the thermal fluctuations. The power spectrum itself does not involve a DWF. The λ renormalization of the inelastic scattering comes "on top" of the expected renormalization of the *po-*

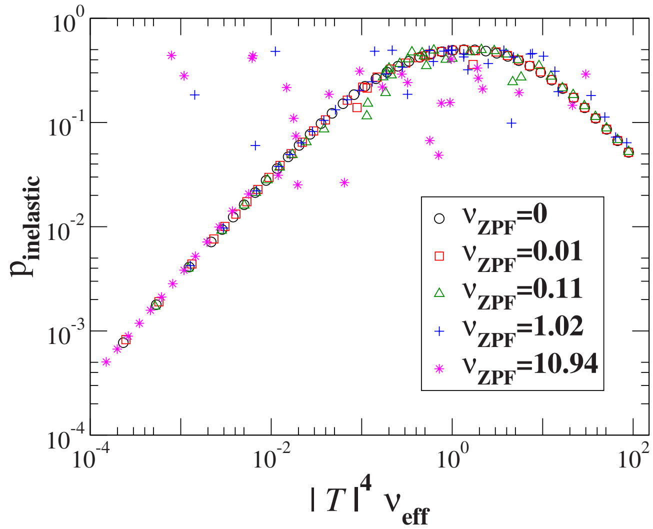

FIG. 8. (Color online) The inelastic cross section $p_{\text{inelastic}}$ versus the scaled intensity of the thermal fluctuations $|\mathcal{T}|^4\nu_{\text{eff}}$, using the data points of Fig. 7.

tential floor and *inertial mass*, which are familiar from the solution of the polaron problem. In our scattering theory framework, the expected renormalization of the potential floor can be deduced from the ZPF induced offset in the effective size of the elastic scatterer (c_S), while the renormalization of the mass comes from the associated energy dependence of the forward scattering amplitude ($\mathcal{T}$).

One can construct an extended bath that consists of a homogeneously distributed set of s scatterers, as described in Ref. 11. This would allow the modeling of a fluctuating environment of physical interest (say a dirty metal environment) with the desired $\tilde{S}(q,\omega)$. In such physical circumstances, we expect a renormalization of (i) the potential floor, (ii) the inertial mass, and (iii) the effective thermal fluctuations. Our results imply that these renormalization effects are nondivergent if the fluctuations are characterized by short range spatial correlations, but still they might modify the low temperature dependence of the dephasing effect.

ACKNOWLEDGMENTS

Part of the derivation in Secs. III and IV was done in collaboration with Sarig.[19] D.C. thanks Ora Entin-Wohlman (BGU) and Joe Imry (Weizmann Inst.) for a discussion that had illuminated the significance of the model in the Debye-Waller perspective. S.B. thanks Grigory Tkachov (MPIPKS) for his interest in this work. The research was supported by the Israel Science Foundation (Grant No. 11/02) and by a grant from the Deutsch-Israelische Projektkooperation (DIP).

[1] B. L. Al'tshuler, A. G. Aronov, and D. E. Khmelnitskii, J. Phys. C **15**, 7367 (1982).
[2] S. Chakravarty and A. Schmid, Phys. Rep. **140**, 193 (1986).
[3] Y. Imry, *Introduction to Mesoscopic Physics* (Oxford University Press, New York, 1997), and references therein.
[4] P. Mohanty, E. M. Jariwala, and R. A. Webb, Phys. Rev. Lett. **78**, 3366 (1997).
[5] D. S. Golubev and A. D. Zaikin, Phys. Rev. Lett. **81**, 1074 (1998); D. S. Golubev and A. D. Zaikin, Phys. Rev. B **59**, 9195 (1999); D. S. Golubev and A. D. Zaikin, arXiv:cond-mat/0512411 (unpublished).
[6] I. L. Aleiner, B. L. Altshuler, and M. E. Gershenson, Waves Random Media **9**, 201 (1999); Phys. Rev. Lett. **82**, 3190 (1999).
[7] D. S. Golubev, G. Schoen, and A. D. Zaikin, J. Phys. Soc. Jpn. **72** (Suppl. A), 30 (2003).
[8] J. von Delft, arXiv:cond-mat/0510563; in *Fundamental Problems of Mesoscopic Physics*, edited by I. V. Lerner, B. L. Altshuler, and Y. Gefen (Kluwer, London, 2004), p. 115.
[9] D. Cohen and Y. Imry, Phys. Rev. B **59**, 11143 (1999).
[10] A. O. Caldeira and A. J. Leggett, Ann. Phys. (N.Y.) **149**, 374 (1983); A. O. Caldeira and A. J. Leggett, Physica A **121**, 587 (1983); A. O. Caldeira and A. J. Leggett, *ibid.* **130**, 374 (1985).
[11] D. Cohen, Phys. Rev. Lett. **78**, 2878 (1997); Phys. Rev. E **55**, 1422 (1997).
[12] D. Cohen, J. Phys. A **31**, 8199 (1998).
[13] F. Guinea, Phys. Rev. B **65**, 205317 (2002).
[14] D. S. Golubev, C. P. Herrero, and A. D. Zaikin, Europhys. Lett. **63**, 426 (2003).
[15] B. Horovitz and P. Le Doussal, Phys. Rev. B **74**, 073104 (2006).
[16] D. Cohen and B. Horovitz, J. Phys. A **40**, 12281 (2007); D. Cohen and B. Horovitz, Europhys. Lett. **81**, 30001 (2008).
[17] F. Marquardt, J. von Delft, R. A. Smith, and V. Ambegaokar, Phys. Rev. B **76**, 195331 (2007).
[18] Y. Imry, arXiv:cond-mat/0202044 (unpublished), and references therein.
[19] C. Sarig, M.Sc. thesis, Ben-Gurion University, 2007.